Microvascular Distribution in the Ocular Conjunctiva and Digestive Tract in an Experimental Setting

Andrius Pranskūnas[1], Vidas Pilvinis[1], Žilvinas Dambrauskas[2], Renata Rasimavičiūtė[1], Eglė Milieškaitė[1], Algimantas Bubulis[3], Vincentas Veikutis[4], Dinas Vaitkaitis[5], E. Christiaan Boerma[6, 7]

[1]Department of Intensive Care, Medical Academy, Lithuanian University of Health Sciences, [2]Department of Surgery, Medical Academy, Lithuanian University of Health Sciences, [3]Center of Mechatronics, Kaunas University of Technology, [4]Institute of Cardiology, Medical Academy, Lithuanian University of Health Sciences, [5]Department of Disaster Medicine, Medical Academy, Lithuanian University of Health Sciences, Lithuania, [6]Department of Intensive Care Medicine, Medical Center Leeuwarden, the Netherlands, [7]Department of Translational Physiology, Academic Medical Center, Amsterdam, the Netherlands

Key Words: *microcirculation; conjunctiva; jejunum; rectum; pigs.*

Summary. *Recently improved microcirculatory imaging techniques, such as orthogonal polarization spectral (OPS) and its technical successor sidestream dark field (SDF) imaging, in handheld devices have allowed a direct observation of the microcirculation at the bedside. Usually a cut-off of 20 μm in diameter is used to differentiate small vessels (mainly capillaries) from large vessels (mainly venules) during this technique. We hypothesized that it was possible to measure the small vessels with a considerably smaller inner diameter.*

Material and Methods. Images of the sublingual, conjunctival, jejunal, and rectal mucosa microcirculation were obtained with SDF videomicroscopy (Microscan®, Microvision Medical, Amsterdam, the Netherlands). Using the validated software, the length and diameter of microvessels were manually traced with a computer-generated line. All vessels were divided into the groups according to the inner diameter.

Results. A total of 156 SDF images of the sublingual, ocular conjunctival, jejunal, and rectal mucosa were taken in 13 pigs. The length of microscopic vessels progressively increased with a decrease in the vessel diameter less than 8 mm in all the lodges, such as sublingual (80.6% of total vessel length), ocular conjunctival (76.5% of total vessel length), jejunal (99.8% of total vessel length), and rectal (97.8% of total vessel length), due to capillary network formation. There was no significant difference in the distribution of vessels from 0 to 10 μm in diameter comparing sublingual and eye conjunctival as well as jejunal and rectal mucosa.

Conclusion. In pigs, small-diameter microscopic vessels (<10 μm) dominated in all the studied lodges (sublingual, ocular conjunctival, jejunal, and rectal mucosa), and this is evidence to establish a new cut-off for capillaries in microcirculatory analysis of SDF imaging in experimental and clinical studies.

Introduction

The microcirculation is a vital part of blood circulation responsible for the transportation and exchange of oxygen and others substances, such as nutrients, hormones, and drugs, to tissue cells and to remove their waste products. The microcirculation involves the smallest vessels with a diameter of less than 100 μm, which are not visible with the eye. These microscopic vessels are arterioles, capillaries, and venules. The structure and function of the microcirculation is heterogeneous in different organs and is related to the metabolic (muscles, heart, brain) and functional (intestinal mucosa, kidney) requirements (1). Recently improved microcirculatory imaging techniques, such as orthogonal polarization spectral (OPS) (2) and its technical successor sidestream dark field (SDF) imaging (3), in handheld devices have allowed a direct observation of the microcirculation at the bedside. Despite some differences, both the methods operate based on the principle that emitted green light (wavelength 530 nm) is absorbed by the hemoglobin content in red blood cells. Thus, red blood cells can be seen as black or gray bodies during imaging. The vessel walls are not visualized themselves, so vessels can only be detected by the presence of red blood cells. OPS and SDF techniques have been validated in comparison with intravital videomicroscopy (4, 5) or nailfold capillaroscopy (6) and can be used only on organs covered by a thin epithelial layer, mostly mucosal surfaces. Nevertheless, these methods are validated during isovolumic hemodilution and at low hematocrits, and this reduces the impact of the number of erythrocytes per capillary with respect to the calculation of capillary diameter (4).

Correspondence to A. Pranskūnas, Department of Intensive Care, Medical Academy, Lithuanian University of Health Sciences, Eivenių 2, 50028 Kaunas, Lithuania
E-mail: a.pranskunas@gmail.com

Another problem arising from the fact that vessel walls are not visualized directly with these techniques is to distinguish venules from capillaries. Usually a cut-off of 20 μm in diameter is used to differentiate small vessels (mainly capillaries) from large vessels (mainly venules) during OPS or SDF imaging analysis (7). Eliminating venules from analysis may help perform a more accurate assessment of the capillaries in specific organs in humans and experimental animals. The knowledge about the distribution of vessels according to diameter in specific organ lodges may help establish a more accurate cut-off diameter for the separation of capillaries from other vessels in an experimental setting and correctly transpose the experimental data of the microcirculation to clinical practice.

The aim of this study was to evaluate and compare the microvascular distribution according to the inner diameter using SDF imaging in the mucosa (ocular conjunctival, sublingual, jejunal, and rectal) of readily accessible organs in pigs under physiological conditions.

Material and Methods

Animals were treated following the guidelines for the care and use of experimental animals of our institution in accordance to applicable laws. The study protocol was approved by the Lithuanian Animal Ethics Committee.

Lithuanian white pigs fasted 12 hours before the experiment, but were allowed free access to water. All the pigs were premedicated with intramuscular ketamine hydrochloride (20 mg/kg) and xylazine (2 mg/kg) followed by cannulation of an ear vein. Orotracheal intubation (tracheal tubes 6.5–7.5 mm in diameter) was performed after the intravenous induction of general anesthesia with thiopental sodium (6 mg/kg). The animals were ventilated using a volume-controlled mode with a positive-end expiratory pressure of 5 cm H_2O. Tidal volume was kept at 10–12 mL/kg, and the respiratory rate was adjusted (14–16 breaths per minute) to maintain end-tidal carbon dioxide tension between 35 and 45 mm Hg. General anesthesia and muscle relaxation were maintained with a continuous intravenous infusion of fentanyl (15 μg/kg per hour), midazolam (0.2 mg/kg per hour), and intravenous boluses of pipecuronium bromide as needed. The stomach was emptied with an orogastric tube. The animal's core temperature was monitored via the pulmonary artery catheter and kept at >38.0°C using warmed solutions and heating mattresses. To maintain arterial blood glucose levels between 4.5 and 7 mmol/L, 10% glucose was infused during the whole experiment.

Surgical Procedures. Both femoral veins and the right femoral artery were surgically dissected and catheterized. An arterial catheter was placed into the right femoral artery to measure invasive arterial blood pressure and to obtain blood gases. A standard thermodilution 7F Swan-Ganz catheter (TD-I, B. Braun Medical, Bethlehem, USA) was advanced into the pulmonary artery through an introducer in the right femoral vein. A central vein catheter was introduced into the left femoral vein for the delivery of medications and fluids. A Foley catheter was inserted into the urinary bladder through a small suprapubic incision.

A proximal loop jejunostomy was constructed for the microcirculatory assessment through 5- to 7-cm incision on the right side of the abdominal wall. The jejunostomy was covered with a moisturized gauze with a local hourly administration of a saline solution to maintain viable mucosa.

A Ringer's lactate solution was infused at a rate of 5 mL/kg per hour during the surgical procedures. After surgical preparations, the animals were allowed to stabilize for 1 hour before recording the baseline measurements.

Protocol and Measurements. After the preparation and stabilization periods, the measurements of the systemic hemodynamics and microcirculation were performed, and blood samples were drawn.

Systemic hemodynamic measurements included systemic, pulmonary arterial, right atrial, and pulmonary artery occlusion pressure and cardiac output measured by the thermodilution technique. Derived hemodynamic variables were calculated according to the usual formulas and indexed for body surface area. Arterial blood samples were obtained for the measurements of hemoglobin, hematocrit, potassium, arterial lactate, and arterial blood gases (ABL 500; Radiometer, Copenhagen, Denmark).

After the experiment, the pigs were euthanized with a bolus injection of thiopental sodium and KCl.

Videomicroscopic Measurements and Analysis. Images of the sublingual, conjunctival, jejunal and rectal microcirculation were obtained with SDF videomicroscopy (Microscan®, Microvision Medical, Amsterdam, the Netherlands) with a ×5 optical probe and ×380 on-screen magnification (3). Unlike OPS imaging, which is based on cross polarization, dark field illumination by concentrically placed green light-emitting diodes is used in SDF imaging. Pulsed green illumination is in synchrony with the camera frame rate to improve the imaging of moving structures such as flowing red blood cells and motion-induced blurring of capillaries (3).

After a gentle removal of saliva and other secretions with isotonic saline-drenched gauze, the device was applied to the sublingual region, avoiding pressure artifacts by establishing a threshold-image. The ocular conjunctiva of the eye was washed with a 0.9% saline solution before the evaluation. An SDF objective with a disposable sterile lens was gently applied to the perilimbal surface of the bulbar conjunctiva, preventing the collapse and drop of flow of

large vessels. Movement artifacts were prevented by attaching the SDF objective to another hand finger placed on the periocular bones and fixating the eyelid. An additional person was often needed to help in establishing the brightness and sharpness of the image. The ocular conjunctiva was regularly rinsed with a 0.9% saline solution to prevent local inflammation and further protected by placing wet gauze on the eye between the measurements. The measurements were performed on the same eye during the whole experiment. The microcirculation of the small intestine was investigated through a jejunostomy by the insertion of the SDF objective into the depth of 5–7 cm from the edge of the stoma and with a slight angulation. The microcirculation of the rectum was investigated through the anus by the insertion of the SDF objective into the depth of 6–10 cm from the edge.

The sublingual mucosa is supplied with blood by the sublingual arteries, which stem from the lingual arteries. The lingual arteries are branches of the external carotid arteries. SDF video microscopy visualizes capillaries and venules in the sublingual mucosa. However, arterioles are usually not visualized due to their location in deeper layers. In the villus of the small intestine in pigs, the central arteriole arborizes into a capillary net at the villus tip. The terminal arterioles can be identified by determining the direction of flow, diameter of the vessel, and characteristic branching into capillaries. In the center of the villus, some capillaries converge into venules (8). The bulbar conjunctiva of the eye is supplied by the anterior ciliary artery and partially by the long posterior ciliary artery. The capillaries in the bulbar conjunctiva form a one-layered bed with hairpin loops and drain to venules disposed underneath the capillary network (9). The rectal mucosal capillaries form a honeycomb-like plexus around the luminal openings of the mucus secreting crypts (Fig. 1).

The sequences of 20 seconds from at least 3 areas were recorded on a hard disk using a personal computer and AVA v3.0 software (Microvision Medi-

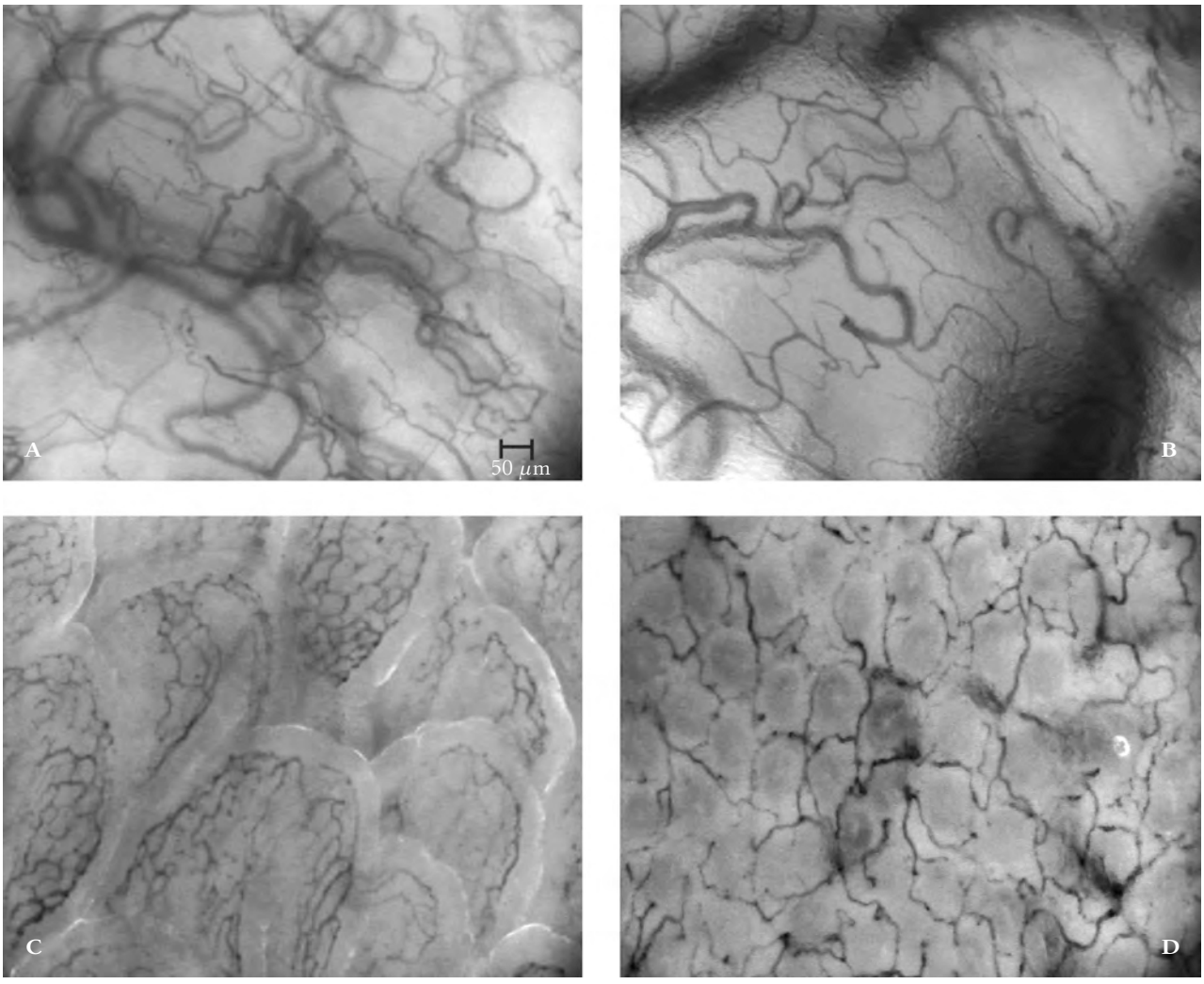

Fig. 1. Digital microphotographs of microcirculation in the sublingual, ocular conjunctival, jejunal, and rectal mucosa
A, sublingual mucosa; B, ocular conjunctival mucosa; C, jejunal mucosa; D, rectal mucosa.

cal, Amsterdam, The Netherlands). Video clips were blindly analyzed offline by 2 investigators in a random order to prevent coupling. Using the validated AVA v3.0 software (10), the length and diameter of microvessels visible in the area were manually traced with a computer-generated line. All vessels were divided into the groups according to the inner diameter. Due to difficulties in the manual tracing of very small vessels, the smallest vessels with a diameter of 0–4 μm were analyzed as one cohort (a pixel spacing of approximately 1.5×1.4 μm) (10). The total line length in mm was then divided by the area to express the microvessel line density as mm/mm^2. The total vessel area was divided by the investigated area and multiplied by 100 to express the vessel surface as a percentage from the total investigated area.

Statistical Analysis. Primary endpoint was the proportion of the total vessel length according to the specific vessel diameter in all investigated lodges. The Statistical Package for Social Sciences (SPSS 15.1 for Windows, Chicago, USA) was used for statistical analysis. Data are presented as mean (SD). Parametric tests were used for comparison within or between the groups with normally distributed variables. For nonnormally distributed variables, nonparametric statistics was employed. A P value of <0.05 was considered statistically significant.

Results

Experimental evaluations were performed in 13 pigs (mean weight, 31.0 kg; SD, 6.2). Systemic hemodynamic and metabolic variables are presented in Table 1. There were no obvious pathological factors that could have an impact on the microcirculation in the studied organs except anesthesia itself.

A total of 156 SDF images were taken: 39 videomicroscopic images for each microvascular lodge of the mucosa of 4 different organs (sublingual, ocular conjunctival, jejunal, and rectal) in 13 pigs. There was no significant difference in the total microscopic vessel length and density comparing the sublingual, ocular conjunctival, and jejunal lodges (Table 2). However, the total vessel length and density in the rectal mucosa was lowest as compared with the sublingual, ocular conjunctival, and jejunal mucosa (P<0.05, ANOVA with post hoc Dunnett test). The evaluation of microscopic vessels was limited in the jejunal and rectal mucosa because of vascular architecture in the small intestine (villi) and the rectum (crypts). Due to an incomplete mechanical contact between the SDF device lens and a rough surface of the jejunum or rectum, it was not possible to fully assess the vascular density and surface. The examples of digital microphotographs in the studied lodges are presented in Fig. 1.

Table 1. Systemic Hemodynamic and Metabolic Variables in Pigs

Variable	Value
HR, beats/min	85 (6)
MAP, mm Hg	100 (16)
MPAP, mm Hg	20 (6)
CI, L/min/m^2	3.5 (0.7)
SVRI, dyne·sec·cm^{-5}/m^2	1966 (308)
P_aO_2, mm Hg	134.5 (30.0)
P_aCO_2, mm Hg	33.7 (3.5)
Arterial pH	7.47 (0.01)
HCO_3, mmol/L	27.1 (0.8)
Lactate, mmol/L	0.9 (0.2)
Hematocrit, %	29 (2)
Glucose, mmol/L	5.1 (1.0)
Temperature, °C	38.5 (0.5)

Values are mean (standard deviation).
HR, heat rate; MAP, mean arterial pressure; MPAP, mean pulmonary artery pressure; CI, cardiac index; SVRI, systemic vascular resistance index.

Figs. 2–3 represent the distribution of vessels according to the inner diameter and the total vessel length or the total vessel area.

In the sublingual mucosa, the vessels with an internal diameter of less than 4 μm comprised 40.7% of the total vessel length; those with an internal diameter of less than 8 μm, 80.6%, and with a internal diameter of less than 20 μm, 90.2%. In the ocular conjunctiva, the vessels with an internal diameter of less than 4 μm comprised 39.7% of the total vessel length, those with an internal diameter of less than 8 μm, 76.5%; and with an internal diameter of less than 20 μm, 91.6%. In the jejunal villi and the rectal crypts, the vessels with an internal diameter of less than 4 μm comprised 71.3% and 65.2% of the total vessel length, respectively, and those with an internal diameter of less than 8 μm, 99.8% and 97.8%, respectively. Comparison of the sublingual and conjunctival mucosa reveled no significant difference in the distribution of vessels from 0 to 10 μm in diameter (P>0.05), but there was a significant difference in the distribution of vessels from 10 to 20 μm in diameter (P<0.05). No significant difference was

Table 2. General Characteristics of the Vessels on Images

Variable	Sublingual Mucosa (n=39)	Ocular Conjunctival Mucosa (n=39)	Jejunal Mucosa (n=39)	Rectal Mucosa (n=39)	P (ANOVA)
Total vessel length, mm	28.8 (4.4)*	28.5 (5.0)†	26.3 (5.1)‡	22.9 (3.1)	<0.0001
Total vessel density, mm/mm^2	35.8 (5.7)*	35.5 (5.5)†	32.8 (6.3)‡	28.9 (4.6)	<0.0001
Vessel surface on image, %	26.4 (6.2)*	26.6 (5.4)†	10.6 (2.3)	10.8 (2.2)	<0.0001

Data are mean (standard deviation).
*P<0.05 sublingual vs. jejunal and rectal; †P<0.05 conjunctival vs. jejunal and rectal; ‡P<0.05 jejunal vs. rectal.

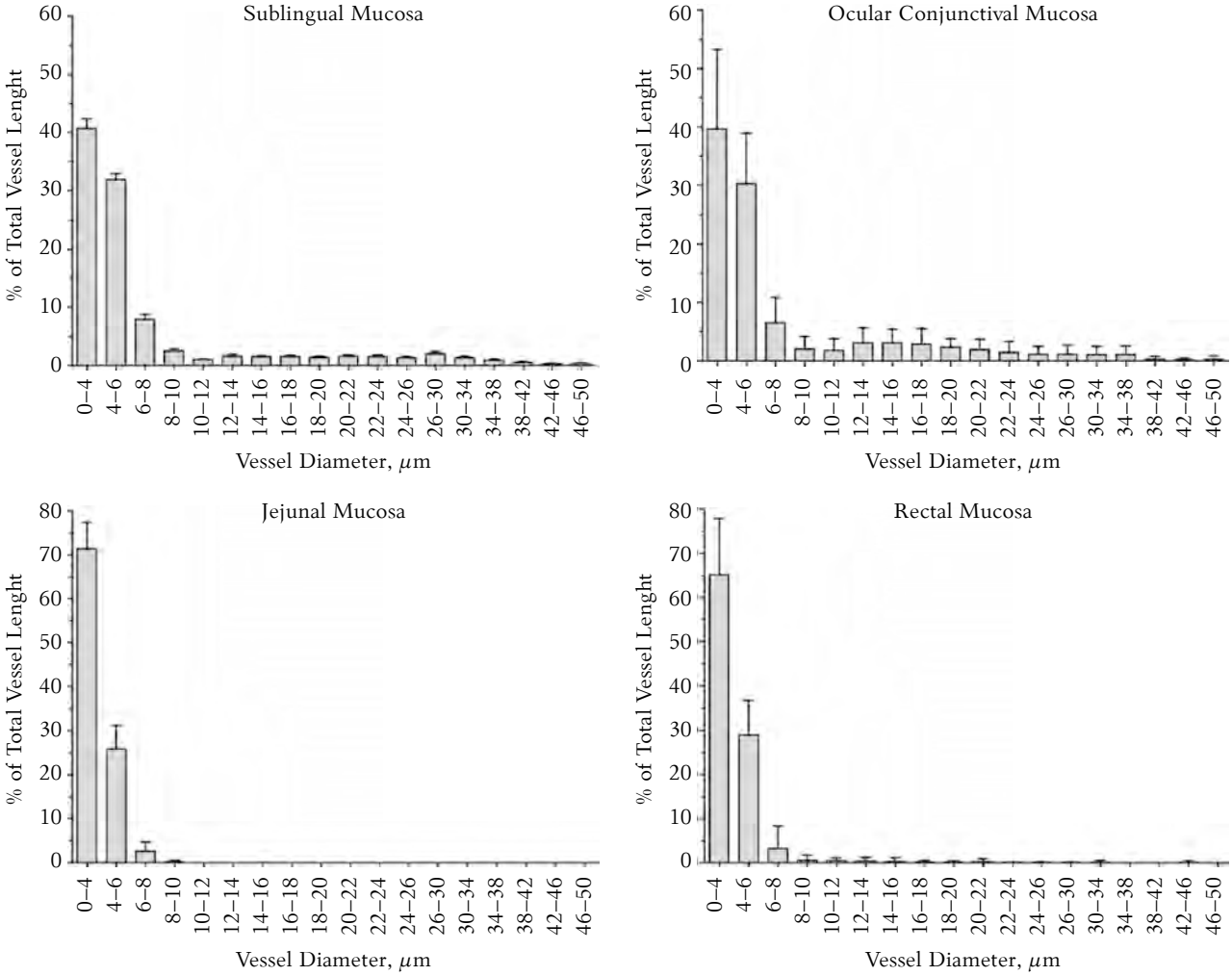

Fig. 2. Distribution of vessels in pigs' sublingual (n=39 images), ocular conjunctival (n=39 images), jejunal (n=39 images), and rectal (n=39 images) mucosa according to the vessel diameter and length

also observed in the distribution of vessels from 0 to 10 μm in diameter between the jejunal and rectal mucosa ($P>0.05$).

Discussion

The aim of this study was to evaluate the microvascular distribution in the mucosa of readily available organs using SDF imaging. Our study showed that the cut-off diameter separating small vessels (mainly capillaries) from other vessels could be more accurate when performing experimental and clinical studies.

We observed no difference in the distribution of vessels from 0 to 10 μm in diameter comparing different vascular lodges. The fact that the length of vessels with a diameter of <8 μm progressively increased, indeed, suggests that vessels from 8 to 10 μm in diameter represent terminal arterioles and collecting venules.

The use of systemic hemodynamic parameters (e.g., mean arterial pressure, cardiac index) is not sufficient to assess the microcirculation (11, 12). Clinical studies have shown that this relatively new method can help predict the outcomes (12, 13) and assess the impact of therapeutic interventions on the microcirculation (14, 15).

A currently used SDF imaging cut-off for a clinical setting is 20 μm (7). According to our clinical data with septic patients (14), in the sublingual region, the vessels with an internal diameter of less than 8 μm comprised 78.2% of the total vessel length; those with an internal diameter of less than 10 μm, 79.2%; and with an internal diameter of less than 20 μm, 92.1% (not published data). This is close to the microvascular distribution in the sublingual mucosa in pigs.

One experimental study using an OPS probe with a ×10 magnification of the objective showed that the majority of microscopic vessels (55%) in the sublingual mucosa were between 5 and 7 μm in diameter, and 96% had an internal diameter of less than 20 μm (16). These results support our findings

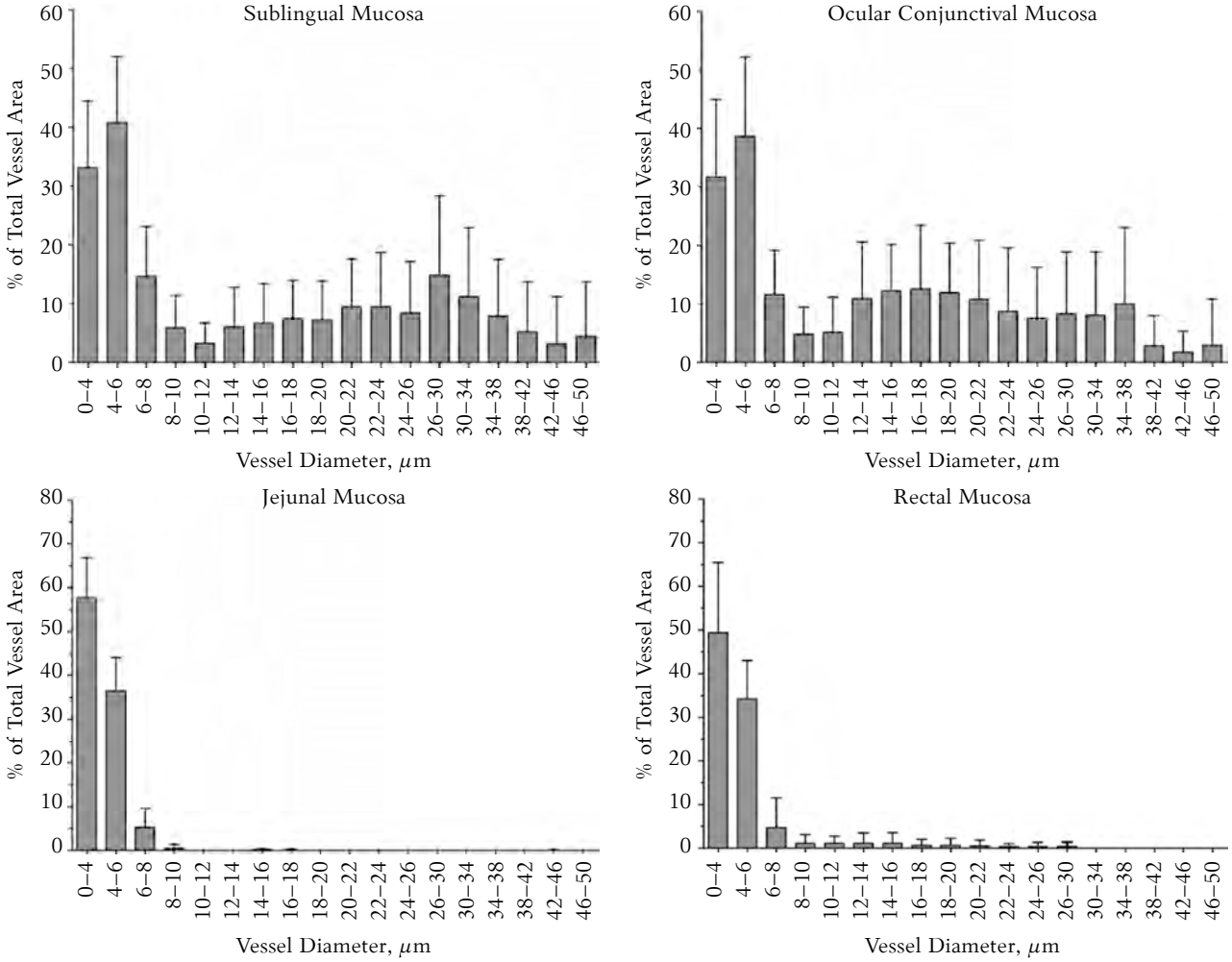

Fig. 3. Distribution of vessels in pigs, sublingual (n=39 images), ocular conjunctival (n=39 images), jejunal (n=39 images), and rectal (n=39 images) mucosa according to the vessel diameter and area

concerning diameters and vessel length. However, our study revealed that a large part of microscopic vessel diameters were less than 4 μm not only in the sublingual, but also in the conjunctival, jejunal, and rectal mucosa.

Our study has some limitations. There may be some differences associated with different technical aspects of the studies. In our study, SDF imaging with a ×5 magnification probe, different grouping according to the diameter, and different validated software for tracing were employed. Capillary contrast and quality of SDF imaging were shown to be considerably better in comparison with OPS (3).

OPS and SDF imaging visualize red blood cells, but not the vessel wall. Therefore, the red cell column diameter is not a true inner diameter of the vessel. Red blood cells flow in the central part of the vessel inner diameter, and there is an additional plasma layer around the red cell column. Some studies have reported that the diameter of the capillary wall is by 38% greater than the diameter of red cell column (17, 18). Interestingly, venous occlusion significantly increased the width of the red cell column by 13%, but no significant increase in the true capillary lumen was observed at the same time (17).

No studies on the microvascular distribution in the rectal mucosa using SDF imaging in pigs have been published before. In our study, the microvascular distribution according to the inner diameter in 4 lodges easy accessible for the experimental evaluation of the microcirculation was compared. We have shown that an actual capillary inner diameter of small vessels (mainly capillaries) in the sublingual, ocular conjunctival, jejunal, and rectal mucosa using SDF imaging is obviously smaller than a published cut-off of 20 μm. The studies by Boerma et al. (19) and De Becker et al. (7) suggested a cut-off value of 20 μm for clinical and experimental studies. The novelty of our study is that it has focused on vessel diameter measurements using the same technique (SDF imaging). Our data are important in performing a more accurate analysis of the mucosal microcirculation, and we suggest reducing the cut-off value to 10 μm.

Conclusions

In pigs, small-diameter microscopic vessels (<10 μm) dominated in all studied lodges (sublingual, ocular conjunctival, jejunal, and rectal mucosa), and this is evidence to establish a new cut-off for capillaries in microcirculatory analysis of SDF imaging in experimental and clinical studies.

Statement of Conflict of Interest

The authors state no conflict of interest.

References

1. den Uil CA, Klijn E, Lagrand WK, Brugts JJ, Ince C, Spronk PE, et al. The microcirculation in health and critical disease. Prog Cardiovasc Dis 2008;51(2):161-70.
2. Groner W, Winkelman JW, Harris AG, Ince C, Bouma GJ, Messmer K, et al. Orthogonal polarization spectral imaging: a new method for study of the microcirculation. Nat Med 1999;5(10):1209-12.
3. Goedhart P, Khalilzada M, Bezemer R, Merza J, Ince C. Sidestream Dark Field (SDF) imaging: a novel stroboscopic LED ring-based imaging modality for clinical assessment of the microcirculation. Opt Express 2007;15(23):15101-14.
4. Harris AG, Sinitsina I, Messmer K. Validation of OPS imaging for microvascular measurements during isovolumic hemodilution and low hematocrits. Am J Physiol Heart Circ Physiol 2002;282(4):H1502-9.
5. Harris AG, Sinitsina I, Messmer K. The Cytoscan Model E-II, a new reflectance microscope for intravital microscopy: comparison with the standard fluorescence method. J Vasc Res 2000;37(6):469-76.
6. Mathura KR, Vollebregt KC, Boer K, De Graaff JC, Ubbink DT, Ince C. Comparison of OPS imaging and conventional capillary microscopy to study the human microcirculation. J Appl Physiol 2001;91(1):74-8.
7. De Backer D, Hollenberg S, Boerma C, Goedhart P, Buchele G, Ospina-Tascon G, et al. How to evaluate the microcirculation: report of a round table conference. Crit Care 2007;11(5):R101.
8. Bellamy JE, Latshaw WK, Nielsen NO. The vascular architecture of the porcine small intestine. Can J Comp Med 1973;37(1):56-62.
9. Ninomiya H, Inomata T. Microvascular anatomy of the pig eye: scanning electron microscopy of vascular corrosion casts. J Vet Med Sci 2006;68(11):1149-54.
10. Dobbe JG, Streekstra GJ, Atasever B, van Zijderveld R, Ince C. Measurement of functional microcirculatory geometry and velocity distributions using automated image analysis. Med Biol Eng Comput 2008;46(7):659-70.
11. De Backer D, Dubois MJ, Schmartz D, Koch M, Ducart A, Barvais L, et al. Microcirculatory alterations in cardiac surgery: effects of cardiopulmonary bypass and anesthesia. Ann Thorac Surg 2009;88(5):1396-403.
12. De Backer D, Creteur J, Preiser JC, Dubois MJ, Vincent JL. Microvascular blood flow is altered in patients with sepsis. Am J Respir Crit Care Med 2002;166(1):98-104.
13. Trzeciak S, Dellinger RP, Parrillo JE, Guglielmi M, Bajaj J, Abate NL, et al. Early microcirculatory perfusion derangements in patients with severe sepsis and septic shock: relationship to hemodynamics, oxygen transport, and survival. Ann Emerg Med 2007;49(1):88-98.
14. Pranskunas A, Vellinga NA, Pilvinis V, Koopmans M, Boerma EC. Microcirculatory changes during open label magnesium sulphate infusion in patients with severe sepsis and septic shock. BMC Anesthesiol 2011;11:12.
15. Boerma EC, Koopmans M, Konijn A, Kaiferova K, Bakker AJ, van Roon EN, et al. Effects of nitroglycerin on sublingual microcirculatory blood flow in patients with severe sepsis/septic shock after a strict resuscitation protocol: a double-blind randomized placebo controlled trial. Crit Care Med 2010;38(1):93-100.
16. Verdant CL, De Backer D, Bruhn A, Clausi CM, Su F, Wang Z, et al. Evaluation of sublingual and gut mucosal microcirculation in sepsis: a quantitative analysis. Crit Care Med 2009;37(11):2875-81.
17. Mahler F, Nagel G, Saner H, Kneubühl F. In vivo comparison of the nailfold capillary diameter as determined by using the erythrocyte column and FITC-labelled albumin. Int J Microcirc Clin Exp 1983;2(2):147-55.
18. Brülisauer M, Bollinger A. Measurement of different human microvascular dimensions by combination of videomicroscopy with Na-fluorescein (NaF) and indocyanine green (ICG) in normals and patients with systemic sclerosis. Int J Microcirc Clin Exp 1991;10(1):21-31.
19. Boerma EC, Mathura KR, van der Voort PH, Spronk PE, Ince C. Quantifying bedside-derived imaging of microcirculatory abnormalities in septic patients: a prospective validation study. Crit Care 2005;9(6):R601-6.

Received 30 January 2012, accepted 30 August 2012